

Modeling and Control of the Silicon Production Process System Using Robust Inventory Control Strategy

Jin Wang

Department of Chemical Engineering
West Virginia University Institute of
Technology

405 Fayette Pike, Montgomery, WV 25136

jin.wang@mail.wvu.edu

Erik B. Ydstie

Department of Chemical Engineering
Carnegie Mellon University
5000 Forbes Ave., Pittsburgh, PA

ydstie@andrew.cmu.edu

Abstract—This paper describes a simplified mathematical model of a silicon production system. We also describe a parameter estimation procedure and reliable control strategy for robust control of the silicon production process. This adaptive extremum-referring control scheme for the silicon reactor process utilizes the steady state production curve to construct a seeking method that drives the silicon production achieving optimization indirectly.

I. INTRODUCTION

The fundamental drawbacks of current modelling and adaptive control techniques for the silicon production process, is that currently available PDE and ODE models and their nonlinear control laws are difficult to derive and apply on-line. There is a large number of unknown parameters, high dimensional state vector, limited number of measurements and system uncertainties, make the model unsuitable for practical application.

In this study, we develop a simple mathematical model and an easily implementable control strategy for the silicon production system. Silicon production is based on carbothermic reduction of silicon dioxide in large plasma arc furnace and subsequent refining for silicon aluminum alloys and micro-electronics applications. The model we develop displays two essential characteristics of the dynamic behavior of the process. The first is that process is not controllable at the operation point of interest. The second is that the process exhibits non-minimum phase behavior. We develop an adaptive control strategy for the nonlinear process system using Lyapunov stability theory and sliding mode control. This gives an adaptive system which is stable and robust with respect to a large class of model plant mismatch and additive noise. This alternative robust control method, based on sliding mode control, is applied to the Silicon Process Model, which is an intrinsically nonlinear and uncertain multiple-input-multiple output plant. Model inversion is not required like nonlinear input-output linearization, to avoid the possible amplification of additive measurement disturbances which may result from inversion of the output nonlinearity. Another advantage of this method is that, we don't need to consider the non-minimum phase behavior exhibit in the complex nonlinear system since the zero dynamic [1], [2] information is not needed in the control strategy, and the robust stabilizing sliding mode control law

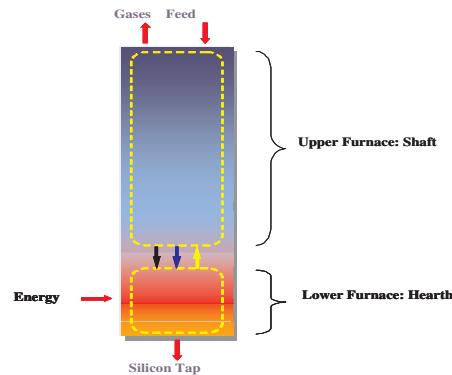


Fig. 1. Shaft-Hearth

adopted guarantees the closed-loop system globally stable.

The motivation in studying the adaptive silicon process control stems from several considerations.

- The full scale model of the process is based on a set of partial differential equations. This makes it difficult to develop a practical control strategy with guaranteed stability properties.
- Considering the system uncertainties caused by modelling error, and unmeasured disturbances, we employ a robust inventory control strategy using sliding mode control.
- The model parameters are learned adaptively based on minimizing a quadratic performance index. Then the stability analysis of the adaptive control system is presented based on Lyapunov theory.

Simulation experiments using industrial off-line data shows that the proposed model and adaptive control method can effectively control the nonlinear silicon system.

II. SILICON PROCESS MODEL

The Mathematical Models of the Silicon Smelting Reactor are too complicated to be effectively used for on line application [3]. The aim of this section is to give a simplified mathematical description of the behavior of the Silicon Smelting Reactor.

The behavior in the reactor can be approximated reasonably well with two sets of spatially distributed reactions

shown in Fig.1: in shaft(upper zone) and in hearth(lower zone). This approach is justified with the following reasons: The shaft zone is cooler and the chemistry network differs from the one in the hotter hearth. The shaft primarily acts as a SiC producer by capturing the Si from the raising gases, which emanate from the hearth. The hearth utilizes SiC and melted SiO₂ to produce Si metal, and SiO and CO gases.

A submerged electric arc/plasma provides the heat for reaction in the lower zone. The products of reaction are liquid Si metal, gaseous SiO and CO. These gases rise to the upper zone providing necessary heat and material for reactions in shaft.

The configuration of the reaction scheme is cyclic in nature; each zone requires the products from the other zone in order to sustain the production of silicon metal. Unreacted SiO and CO gases leave the furnace and are oxidized with air. CO₂ gas is emitted to the atmosphere while the particulate SiO₂ is captured and prepared for further processing and delivery to concrete manufactures. The silicon metal is recovered or tapped from the furnace during regular intervals, giving the process a semi-batch nature. To maintain an even distribution of reactants and eliminate any undesired gas cavities, the furnace is stoked. Stoking is imposed on the system by intermittently mechanically pressing and breaking the partially reacted crusted charge downward using a paddle-type device.

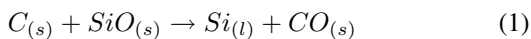
The process is energy intensive and the necessary power is delivered in the form of high-current electrical energy through carbon electrodes submerged in the charge burden. The number of electrodes varies from three to six in most applications. Several modes of heat generation and transfer contribute to furnace operation. A part of the electrode current flows through the charge in the upper furnace, and its resistance is responsible for Ohmic heating of the charge material in the upper furnace. Radiation effects become significant toward the submerged tip of the electrode where arcing takes place. An arc is a flow of electrons, which discharges large amounts of energy due to plasma resistance. The intense arcing induces natural stirring and convection is the primary mode of heat distribution in the lower, hot zone of the furnace [4]. Recent experimental studies on an industrial size furnace indicate that approximately 60% of input energy is distributed in the upper furnace zone while the remaining 40% is transferred via the arc in the lower furnace.

Based on the above analysis, the chemical reactions and the material balance in both zone are described as follows.

A. Chemical Reaction and Model of the Process

The analytical model, obtained by mass balance principle to the chemical reaction processes, is given as:

In Shaft: Chemical reaction,



The process model is given,

$$V_s \frac{dC_c^s}{dt} = F_c^s - V_s r_s \quad (2)$$

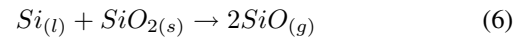
$$V_s \frac{dC_{si}^s}{dt} = -F_{si}^s + V_s r_s \quad (3)$$

$$V_s \frac{dC_{sio}^s}{dt} = F_{sio}^h - V_s r_s - F_{sio}^p \quad (4)$$

$$V_s \frac{dC_{co}^s}{dt} = -F_{co}^p + V_s r_s \quad (5)$$

where $r_s = k_s C_c^s C_{sio}^s$.

In Hearth: Chemical reaction,



The process model is given,

$$V_h \frac{dC_{sio}^h}{dt} = -F_{sio}^h + 2V_h r_h \quad (7)$$

$$V_h \frac{dC_{sio2}^h}{dt} = F_{sio2}^h - V_h r_h \quad (8)$$

$$V_h \frac{dC_{si}^h}{dt} = F_{si}^s - F_{si}^p - V_h r_h \quad (9)$$

where $r_h = k_h C_{si}^h C_{sio2}^h$.

In the above equations, the flows are given,

$$F_{si}^s = k_1 C_{si}^s \quad (10)$$

$$F_{co}^s = k_2 C_{co}^s \quad (11)$$

$$F_{si}^p = k_3 C_{si}^h \quad (12)$$

$$F_{sio}^h = k_4 C_{sio}^h \quad (13)$$

$$F_{sio}^p = k_5 C_{sio}^s \quad (14)$$

C_i^j denotes the concentration of i in the reaction of j , ($j = shaft/hearth$). And $k_1, k_2, k_3, k_4, k_5, k_s, k_h$ are reaction rate constants to be determined experimentally. V_s, V_h are two volumes in shaft and hearth. Reasonably, an important physical assumption, which concerns the energy in the reactor, is that the volumes (V_h and V_s) are proportional to the effective areas, and the effective areas are proportional to the power, we have,

$$V_h = A_{eff}^h h_h = k^h p h_h \equiv \theta_h p \quad (15)$$

$$V_s = A_{eff}^s h_s = k^s p h_s \equiv \theta_s p \quad (16)$$

where p denotes the power supplied in the furnace; h_h and h_s are height of hearth and shaft respectively; k^h and k^s are proportional factors of hearth and shaft respectively; θ_h and θ_s are two lumped parameters which will be learned based on the system output.

In Steady State: From the model equations, we are able

$k_s = 50$	$k_h = 3$	$k_1 = 120$	$k_2 = 80$	$k_3 = 80$
$k_4 = 180$	$k_5 = 55$			

TABLE I
MODEL PARAMETERS

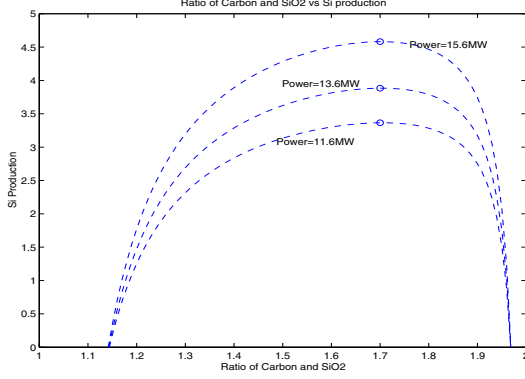


Fig. 2. Production Curve with Different Power

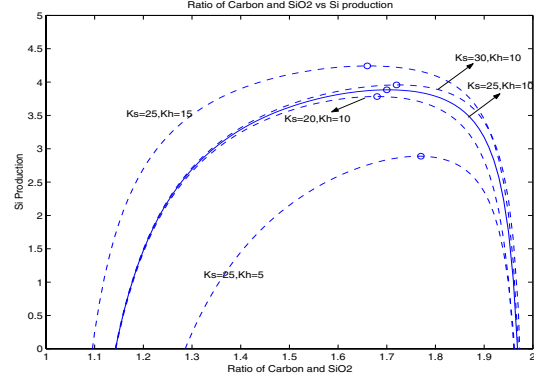


Fig. 3. Production Curve with Different parameters k_s, k_h

$$\begin{aligned} x_7 &= C_{si}^h \\ u_1 &= F_c^s \\ u_2 &= F_{sio2}^h \end{aligned}$$

The system becomes:

$$\frac{dx_1}{dt} = \frac{u_1}{V_s} - k_s x_1 x_3 \quad (24)$$

$$\frac{dx_2}{dt} = -\frac{k_1 x_2}{V_s} + k_s x_1 x_3 \quad (25)$$

$$\frac{dx_3}{dt} = \frac{k_4 x_5}{V_s} - k_s x_1 x_3 - \frac{k_5 x_3}{V_s} \quad (26)$$

$$\frac{dx_4}{dt} = -\frac{k_2 x_4}{V_s} + k_s x_1 x_3 \quad (27)$$

$$\frac{dx_5}{dt} = -\frac{k_4 x_5}{V_h} + 2k_h x_7 x_6 \quad (28)$$

$$\frac{dx_6}{dt} = \frac{u_2}{V_h} - k_h x_7 x_6 \quad (29)$$

$$\frac{dx_7}{dt} = \frac{k_1 x_2}{V_h} - \frac{k_3 x_7}{V_h} - k_h x_7 x_6 \quad (30)$$

And the system outputs are defined as the total mass M_{tot} and the total carbon M_c .

$$M_{tot} = V_s(x_1 + x_2 + x_3 + x_4) + V_h(x_5 + x_6 + x_7) \quad (31)$$

$$M_c = V_s(x_1 + x_4) \quad (32)$$

In steady state,

$$\begin{aligned} x_1 &= \frac{u_1 k_5}{V_s k_s (2u_2 - u_1)} \\ x_2 &= \frac{u_1}{k_1} \\ x_3 &= \frac{2u_2 - u_1}{k_5} \\ x_4 &= \frac{u_1}{k_2} \\ x_5 &= \frac{2u_2}{k_4} \\ x_6 &= \frac{u_2 k_3}{V_h k_h (u_1 - u_2)} \end{aligned}$$

to solve the states in the steady state.

$$C_{si}^s = F_c^s / k_1 \quad (17)$$

$$C_{si}^h = (F_c^s - F_{sio2}^h) / k_3 \quad (18)$$

$$C_{sio}^h = 2 * F_{sio2}^h / k_4 \quad (19)$$

$$C_{sio}^s = (2F_{sio2}^h - F_c^s) / k_5 \quad (20)$$

$$C_c^s = F_c^s / (V_s * k_s * C_{sio}^s) \quad (21)$$

$$C_{co}^s = F_c^s / k_2 \quad (22)$$

$$C_{sio2}^h = F_{sio2}^h / (V_h * k_h * C_{si}^h) \quad (23)$$

Given a total mass M_{tot} , let $u_1 = F_c^s$ and $u_2 = F_{sio2}^h$. ratio of $u_1/u_2 = ratio$. We can plot the Si production v.s. the ratio at steady state. We call this plot production curve, which can show the maximum Si production under the input ratio of u_1 and u_2 . Fig.2 shows the production curve under three different power inputs. Fig.3 shows the the production curve under different parameters k_s and k_h . These two figures clearly show the relationship between the parameters or power and the maximum of the Si production. In our study, the model parameters are set in Table I. And the two volume V_h and V_s will be learned in the parameter estimation.

B. Formulation of Nonlinear Control Problem:

Let

$$\begin{aligned} x_1 &= C_c^s \\ x_2 &= C_{si}^s \\ x_3 &= C_{sio}^s \\ x_4 &= C_{co}^s \\ x_5 &= C_{sio}^h \\ x_6 &= C_{sio2}^h \end{aligned}$$

$$x_7 = \frac{u_1 - u_2}{k_3}$$

III. GRADIENT FLOW PARAMETER ESTIMATION

The silicon production and the SiO obtained from the model are given as,

$$\begin{aligned} y_1 &= V_h x_7 \\ y_2 &= V_s x_3 \end{aligned}$$

Define an objective function

$$J = \frac{1}{2}(y_1 - y_1^*)^2 + \frac{1}{2}(y_2 - y_2^*)^2 \quad (33)$$

where y_1^* is the measurement of silicon production, and y_2^* is the measurement of dust(SiO).

Define the parameter set, $\theta = [\theta_h, \theta_s]^T$. To min J , use the following parameter adaptation law,

$$\dot{\theta} = -\eta \frac{\partial J}{\partial \theta} \quad (34)$$

such, the two parameters are updated by

$$\begin{aligned} \dot{\theta}_h &= -\eta \frac{\partial J}{\partial \theta_h} \approx -\eta(y_1 - y_1^*)p \frac{u_1 - u_2}{k_3} \\ \dot{\theta}_s &= -\eta \frac{\partial J}{\partial \theta_s} \approx -\eta(y_2 - y_2^*)p \frac{2u_2 - u_1}{k_5} \end{aligned} \quad (35)$$

where η is a learning rate. Here we substituted the steady states into the adaptation law instead of the dynamic states, since it is conveniently lumped together with the other parameters. Such an approximation might, however, slow down the speed of convergence in finding optimal solutions. But since the states are not measured, this is a compromising approximation way.

In this way, the Lyapunov function (33) will converge since,

$$\begin{aligned} \frac{d}{dt} J &= \frac{\partial J}{\partial \theta} \frac{\partial \theta}{\partial t} \\ &= \frac{\partial J}{\partial \theta_h} \dot{\theta}_h + \frac{\partial J}{\partial \theta_s} \dot{\theta}_s \\ &= -\eta \left(\frac{\partial J}{\partial \theta_h} \right)^2 - \eta \left(\frac{\partial J}{\partial \theta_s} \right)^2 \leq 0 \end{aligned} \quad (36)$$

IV. INVENTORY CONTROL STRATEGY DESIGN FOR THIS PROCESS

Inventory control strategy is first introduced in [5] and then successfully applied to chemical process control systems. To deal with system uncertainties, a sliding mode inventory control strategy is presented in [6].

In our application, choose the objective inventory function $v = [v_1, v_2]^T = [M_{tot}, M_c]^T$, and the reference vector $v^* = [v_1^*, v_2^*]^T = [M_{tot}^*, M_c^*]^T$. The inventory dynamic equations can be obtained from the dynamic model and (31, 32).

$$\begin{aligned} \frac{dM_{tot}}{dt} &= u_1 + u_2 - k_5 x_3 - k_2 x_4 - k_3 x_7 \equiv f_{tot}(u, x, \theta) \\ \frac{dM_c}{dt} &= u_1 - k_2 x_4 \equiv f_c(u, x, \theta) \end{aligned}$$

then the inventory dynamic balance can be written as,

$$\dot{v} = f(u, x, \theta) = f(u, x, \hat{\theta}) + \Delta \quad (37)$$

where $f(u, x, \theta) = [f_{tot}(u, x, \theta), f_c(u, x, \theta)]^T$; $\hat{\theta}$ is the parameter estimate; Δ is the lumped uncertain term caused by the parameter estimate and other disturbance, clearly Δ is bounded, i.e. $\|\Delta\| \leq \delta$, δ is a constant.

Define a sliding surfaces, $S(t) = [S_{tot}(t), S_c(t)]^T$,

$$\begin{aligned} S_{tot}(t) &= \left(\frac{d}{dt} + k_0 \right) \int_0^t e_{tot}(\tau) d\tau = 0, \quad S_{tot}(0) = 0 \\ S_c(t) &= \left(\frac{d}{dt} + k_0 \right) \int_0^t e_c(\tau) d\tau = 0, \quad S_c(0) = 0 \end{aligned} \quad (38)$$

where $e_{tot} = M_{tot} - M_{tot}^*$, and $e_c = M_c - M_c^*$. According to the sliding mode inventory control strategy [6], the control law equation:

$$f(u, x, \hat{\theta}) = -k_0(v - v^*) + \dot{v}^* - \hat{\delta} \text{sgn}(S(t)) \quad (39)$$

where $\hat{\delta}$ is the estimate of δ . We will use the following adaptation algorithm for the bound of δ

$$\dot{\hat{\delta}} = \alpha \|S(t)\| \quad (40)$$

where α is a positive constant.

Such, the control law will be obtained by:

$$\begin{aligned} u_1 + u_2 &= k_5 x_3 + k_2 x_4 + k_3 x_7 - k_0^{tot}(e_{tot}) \\ &\quad - \hat{\delta}_{tot} \text{sgn}(S_{tot}(t)) \end{aligned} \quad (41)$$

$$u_1 = k_2 x_4 - k_0^c(e_c) - \hat{\delta}_c \text{sgn}(S_c(t)) \quad (42)$$

The advantage of this sliding mode control strategy is that it can effectively handle complicated nonlinear plants with uncertainties the system uncertainties caused by modelling error, parameters estimation, immeasurable disturbance and etc.. Good performance, simple structure and easily understanding adjusted parameters make the strategy attractive to industrial application. The closed loop system analysis and stability proof can be found in [6].

V. MODELLING AND CONTROL SIMULATION RESULTS

To study the effectiveness of the silicon process model and the control strategy we proposed for the Si production process, a simulation study is performed using real furnace data in the Norway Elkem metal Co.. The system inputs and outputs match results are shown in Fig.4, Fig.5 and Fig.6. It is worth noting that there are so many big uncertainties in the electric arc furnace system, such as, long time delay, Si production tapping period, measurement errors, known system parameters, modelling errors and so on, therefore, the matching errors are bigger. But the average values are approximately near. The ratio of carbon and quartz is shown in Fig.7. The two learning parameters are shown in Fig.8.

In this application, our control objective is to seek the extremum of Si production by feeding the Carbon and SiO_2 . For material control of the silicon furnace, process inventories include the holdup of total mass and total carbon

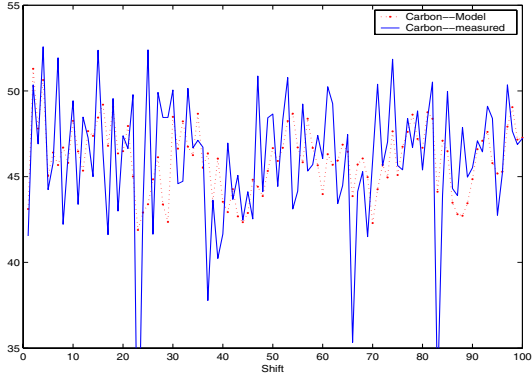


Fig. 4. Carbon

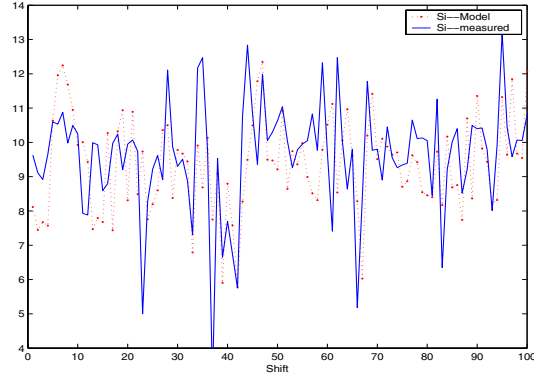


Fig. 6. Si production

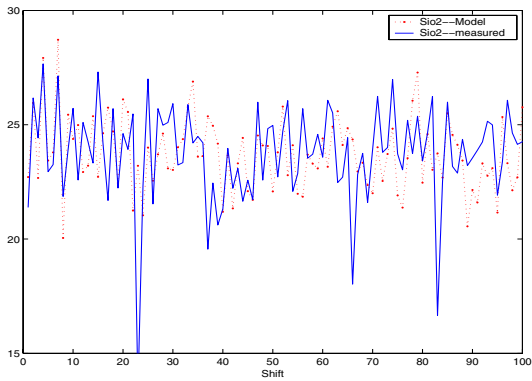


Fig. 5. SiO₂

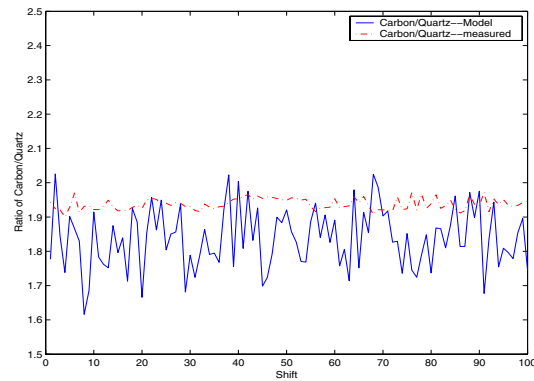


Fig. 7. Ratio of Carbon and Quartz

in the furnace. we are concerned with elemental balance of C and this inventory depends on the sum defined as:

$$M_{C_{tot}} = M_c + M_{C_o}$$

Figure 10 shows a plot of these inventories at various feed ratio $r = Carbon/Quartz$ and which correspond to the Si metal production rate and the total carbon $M_{C_{tot}}$. Using $M_{C_{tot}}$ as the feedback variables therefore gives the same problems as using Si production. This caveat underpins why $M_{C_{tot}}$ is essential, it also yields a monotonic inventory. In this inventory control strategy, inventories are the output variables and their monotonic character does not present similar difficulties to control as do silicon metal.

Motivated by this discussion, the inventory control strategy for the silicon furnace is shown in Fig.9.

The pre-calculation box conducts the two reference signals based on the model. The controller box implements the control strategy we described. The Process box represents the silicon-smelting furnace. The Model box represent the model described above, its parameters are updated with a parameter estimation scheme. When model and process outputs are in accord, model variable are submitted to the inventory variable synthesizer where $M_{C_{tot}}$ and M_{total} are constructed. The necessity for M_{total} is justified by having two control objectives: (1). Control total elemental carbon holdup with carbon feed input. (2). Control overall process

holdup with quartz feed input. The furnace can only hold limited amount of material and to achieve this, the quartz feed is adjust suitably so that the overall mass balance is satisfied.

As we discuss, Si production F_{si}^p is nearly proportional to Total Mass at steady state, in another word, we can control the Si production by controlling the total mass M_{tot} . Fig.10 shows the Si production curve under some fixed total mass and the total carbon curve. In this way, by setting the total mass, we will know the optimal Si production, and the total carbon reference under this optimal Si production point. That is to say, we can determine M_{tot}^* and M_C^* by this Figure.

Fig.11 and 12 show the control response of the total mass and carbon. By control the total mass, we will obtain the maximum Si production.

VI. CONCLUSIONS

In this paper, we review some of the challenges associated with operation and control of the silicon-smelting furnace, and present a simple physical model for this process, and design a good control strategy. This was illustrated with simulations

In this study, the process inventories are total elemental carbon holdup and the total holdup. These process inventories are monotonic and paired with the carbon and

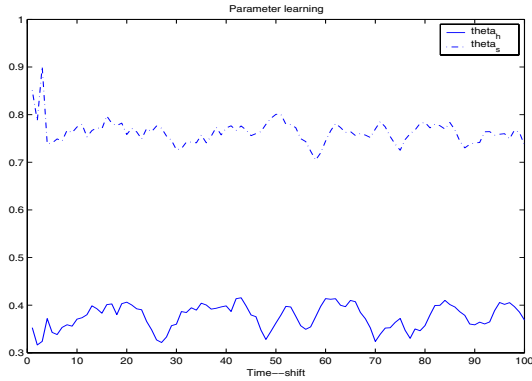


Fig. 8. The two parameters during the learning process θ_h, θ_s

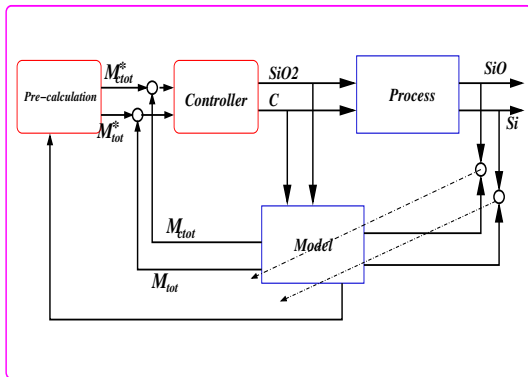


Fig. 9. Control Strategy for the Silicon Process

quartz boundary fluxes, comprise a sign-preserving passive input-output pair. Inventory control strategy as well as simulation-assisted open-loop control strategy simulations were prepared. Under inventory control, process converges to a set point and reaches a desired production rate.

REFERENCES

- [1] A.Isidori. *Nonlinear Control System*. Springer Verlag, New York, 1989.
- [2] J.J.E.Slotine and W.P.Li. *Applied Nonlinear Control*. Prentice Hall, 1991.
- [3] Martin G. Ruzskowski. *Passivity-Based Control of Transport-Reaction Systems: Application to Silicon Production*. Ph.d. dissertation, Carnegie Mellon University, Pittsburgh, PA, 2003.
- [4] A.M.Valderhaug. *Modelling and Control of Submerged-Arc Ferrosilicon Furnaces*. Ph.d. dissertation, NTH, 1992.
- [5] C.A.Farschman K.P.Viswanath and B.E.Ydstie. Process systems and inventory control. *AIChE*, 44(8):1841–1857, August 1998.
- [6] Jin Wang and Erik B. Ydstie. Robust inventory control systems. *Proceedings of the ACC'2004, and IEEE Trans. Syst.,Man,Cybern.-Part B*, pages 3197–3202, June 2004.

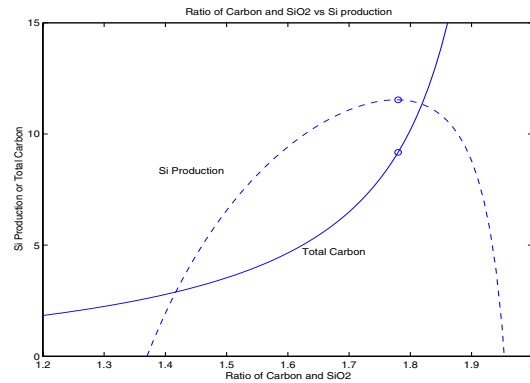


Fig. 10. Production Curve and the Total Carbon Curve

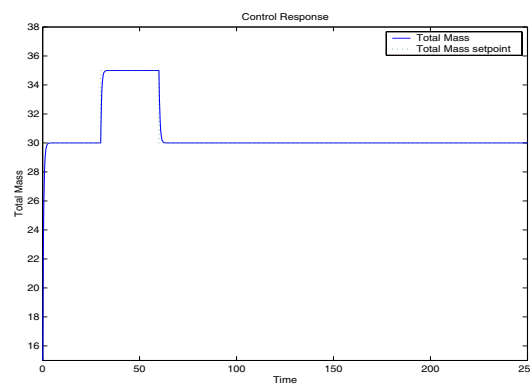


Fig. 11. Control Response of the Total Mass

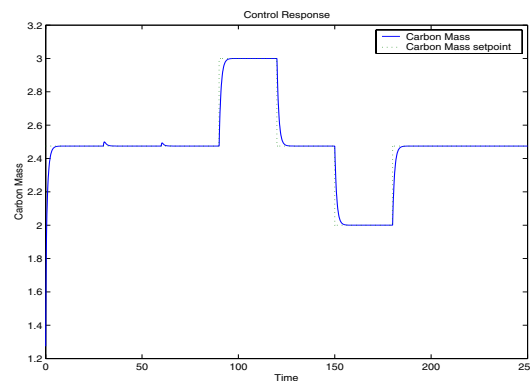


Fig. 12. Control Response of the Total Carbon Mass